Journal of Control, Automation and Electrical Systems (2020) 31:926–934
https://doi.org/10.1007/s40313-020-00602-y

Performance Enhancement of Electrohydraulic Servo System Using Teaching Learning-Based Optimization and CDM-Backstepping with Disturbance Observer

F. Haouari[1] · R. Gouri[1] · N. Bali[2] · M. Tadjine[3] · M. S. Boucherit[3]

Received: 22 November 2018 / Revised: 14 March 2020 / Accepted: 18 April 2020 / Published online: 17 May 2020

Abstract
In this paper, a new application of teaching learning-based optimization algorithm is presented for tuning the parameters of the controller based on disturbance observer with coefficient diagram method and backstepping method for electrohydraulic servo system to compensate the external disturbances and parameter uncertainties. Accurate stability and asymptotic convergence of the tracking errors to zero are achieved. Simulation results are integrated to expose the efficacy and robustness of the proposed approach.

Keywords Electrohydraulic servo system · Backstepping control · Coefficient diagram method controller · Disturbance observer

1 Introduction

Electrohydraulic servo systems (EHSS) are commonly employed in recent engineering applications such as manufacturing equipment, aircrafts, submarine operations and robotic (Detiček and Kastrevc 2016). Compared with their electrical counterparts (Yuan et al. 2018), a good power-to-weight ratio is achieved. However, the EHSS is characterized by highly nonlinear properties rising from square-root flow function (Baek et al. 2018); a great challenges for controller design of EHSS are presented by parameter uncertainties and external disturbances. Several control methods have been implemented for EHSS, the employment of linear method of control is permitted by local linearization of the nonlinear dynamics about a nominal operating form, but the global stability of this technique was not confirmed such that PID control (Yuan et al. 2018). Input–output linearization has been suggested; on the other hand, a high amplitude of control input signal can be acquired due to elimination of the nonlinear terms (Shoja-Majidabad 2016). Sliding mode control was used to control the EHSS, it is robust to modeling error with certain conditions, but the problem of chattering is produced, due to the switching input (Ahn et al. 2014). Variable structure control methods were proposed; however, chattering problem can be produced in the control signal by excitement of high-frequency modes (Ahn et al. 2014). Several backstepping control method using the nonlinear dynamics properties of an EHSS has been suggested and recover the position tracking performance (Ba et al. 2016; Detiček and Kastrevc 2016). However, in these researches, the disturbance elements in terms of the external disturbance were estimated by observer and were not discussed to estimate and compensate the unknown disturbance and uncertainties in order to improve the performance.

Newly, more attention has been won by the disturbance observer-based control for system plants subject to large disturbances and uncertainties due to its faster response in handling the disturbances (Vieira et al. 2017). So far various disturbance observers have been planned for EHSS. In one study, an integral sliding mode disturbance observer was suggested to deal with the problem of load pressure control in the company of the external disturbances (Has et al. 2015), the structure of this controller can be simply applied, and a robust performance is presented where the

✉ F. Haouari
haouari_fouad@yahoo.fr

[1] Laboratory of Innovative Technologies, COSI Team, ENST Ex Biomédical, 16078 Bordj El Kiffan, Algiers, Algeria

[2] Electrical Engineering and Computing Faculty, USTHB, El Alia, P.O Box 32, 16111 Bab Ezzouar, Algiers, Algeria

[3] Department of Electrical Engineering, Process Control Laboratory, ENP , 10 Avenue Hassan Badi, P.O Box 182, 16200 Algiers, Algeria

chattering effect is minimized. In other study (Sheng and Li 2016), a disturbance observer based on hybrid robust control was presented to reject low-frequency disturbance and high-frequency noises, but was employed only for a linear model of the considered system. In other research it was offered a disturbance observer-based backstepping control; however, the high amplitude of the control input signal was affected (Wang and Wang 2017).

In this work, a disturbance observer-based coefficient diagram method CDM was planned (Ali et al. 2019; Coelho et al. 2016; Erkan et al. 2017; Mohamed et al. 2016) and backstepping control (CDM-backstepping) (Arsalan et al. 2018; Dashkovskiy and Pavlichkov 2017) to estimate the disturbance and to increase the position tracking performance in the presence of external disturbances containing friction and load force, while evading amplification of the measurement noise. An auxiliary state variable can be employed to evade the use of the derivative of the measured signal. This approach is arranged among the robust control, and its efficient can be proven for unstable system and nonminimum phase system where the TLBO is another technique for increasing the robustness by finding the optimum parameters. The asymptotic convergence of the tracking error can be guaranteed in the presence of both friction and load force. The performance of the proposed method is validated without any chattering effect via simulations.

It is evident that the performance of controlled system depends not only on controller structure but also on the artificial intelligent technique employed; therefore, proposing new controller approaches by means of high-performance optimization technique such as teaching learning-based optimization (TLBO) is always welcome.

TLBO is a novel nature-inspired algorithm (Chatterjee and Mukherjee 2016; Sahu et al. 2016) and frequently employed in practical optimization problems. Some attractive features was attained and generally applied to get global optimal solutions for optimization problems with a reduced computational cost, but also is simple for having only the number of learners as a parameter comparing with many optimization techniques, such that genetic algorithm, GA, which has three parameters, population size, crossover rate and mutation rate. The same case is with particle swarm optimization PSO where the inertia weight, social and cognitive parameters are employed. Similarly, in artificial bee colony ABC employed, scout and onlookers are required as the parameters; in harmony search, HS, the parameters of harmony memory consideration rate, the pitch-adjusting rate and the number of improvizations are necessitated. A very crucial role in the performance of the algorithms is motivated by the number and the proper selection of these control parameters; this optimization method is achieved by simulating the teaching phase and learning phase. The outcome is related to the performance of the learners and the teacher. In this algorithm, the knowledge is upgraded by the learners on the basis of the teacher knowledge which is known as a highly qualified person. If the student is teaching by the teacher in a well-mannered way, then the outcome of the students will definitely improve. The algorithm works on the principle of preserving the best student as the teacher, and the other functions are improvized on the basis of best solution obtained (Chatterjee and Mukherjee 2016). Here, the effectiveness of the TLBO algorithm is exploited to find the optimum value parameters of CDM-backstepping with disturbances while controlling the EHSS.

The paper is organized as follows. In Sect.2, EHSS state space model is presented. In Sect. 3, the CDM controller is designed for linear system. In Sect. 4, disturbance observer-based CDM-backstepping is proposed. In Sect. 5, the explanation of TLBO algorithm is presented. In Sect. 6, the numerical results and discussion are treated to appear the effectiveness of the proposed control scheme; finally, conclusions are presented in Sect. 7.

2 EHSS State Space Model

The state space model of EHSS is taken 5th order on the way to include an accurate model of dynamic characteristics and so its influence on performance of position control, and it is written as follows

$$\begin{cases} \dot{x}_1 = x_2 \\ \dot{x}_2 = f_1 + \frac{A_p}{m} x_3 - \frac{d}{m} \\ \dot{x}_3 = f_2 + b x_4 \\ \dot{x}_4 = x_5 \\ \dot{x}_5 = f_3 + a_6 u \\ y = x_1. \end{cases} \tag{1}$$

where $x_1(t)$ is the piston position of the hydraulic cylinder, $x_2(t)$ is the piston velocity, $x_3(t)$ is the load pressure of the hydraulic cylinder, $x_4(t)$ is the spool position of the servo valve, $u(t)$ is the input voltage of the servo amplifier, $y(t)$ is the system output, and d is the disturbance in unmodeled friction and load force.

where $f_1 = -(-K_s x_1 - B x_2)/m$, $f_2 = a_2 x_2 + a_3 x_3$, $f_3 = a_4 x_4 + a_5 x_5$, $a_1 = A_p/m$, $a_2 = -4\beta_e A_p V_t$, $a_3 = -4\beta_e C_{tp} V_t$, $a_4 = -{\omega_{sv}}^2$, $a_5 = -2\zeta_{sv}\omega_{sv}$, $a_6 = {\omega_{sv}}^2 K_s K_a$ and $b = \left(-4\beta_e C_d \omega V_t \sqrt{\rho}\right)\sqrt{P_s - \mathrm{sgn}(x_4)x_3}$.

m is the equivalent mass with considerations of the mass of the pistons and the oil in the chambers of the hydraulic cylinder, A_p is the effective pressure area of the piston, V_t is the total actuator volume with consideration of the pipe volume between the servo valve and the hydraulic cylinder, C_d is the discharge coefficient, ρ is the density of hydraulic oil, K_s is the spring stiffness, B is the viscous damping coefficient of the pistons, K_a is the servo amplifier gain, β_e is the effective

volume elasticity modulus of the hydraulic fluid, ω is the area gradient of the servo valve spool, C_{tp} is the total leakage coefficient, P_s is the supply pressure of the pump, ω_{sv} is the servo valve natural frequency, ζ_{sv} is the servo valve damping ratio, and K_{sv} is the torque motor gain.

3 Linear Control Using CDM Design

CDM is one of the algebraic methods with polynomial structure by combining classical and modern control design (Ali et al. 2019), the design of the controller is permitted for the indicated settling time with a good balance in terms of simplicity, minimum overshoot, stability and robustness, and more reliable parameters selection can be designed based on the stability index and equivalent time constant.
For the specified system, the output of the CDM control system as illustrated in Fig. 1 is expressed as

$$y_i = \frac{N(s)F(s)}{P(s)} r_i + \frac{A(s)N(s)}{P(s)} d_i. \tag{2}$$

where y_i is the output, u_i is the input control, r_i is the reference input, d_i is the external disturbance signal, $N(s)$ and $D(s)$ are the numerator and the denominator of the transfer function of the system, respectively, $A(s)$ is the denominator polynomial of the controller transfer function, while $F(s)$ and $B(s)$ are named the reference numerator (prefilter) and the feedback numerator polynomials of the controller transfer function. As well, the characteristic polynomial $P(s)$ is formulated in the following polynomial form (Abtahi and Yazdi 2019; Coelho et al. 2016).

$$\begin{aligned} P(s) &= D(s)A(s) + N(s)B(s) = \sum_{i=0}^{n} \mu_i s^i \\ &= \mu_0 \left[\left\{ \sum_{i=2}^{n} \left(\prod_{j=1}^{i-1} \frac{1}{\gamma_{i-j}^{j}} (T_0 s)^i \right) \right\} + T_0 s + 1 \right] \end{aligned} \tag{3}$$

where $A(s) = \sum_{i=0}^{n} l_i s^i$ and $B(s) = \sum_{i=0}^{n} r_i s^i$, the transient response characteristic is represented by the equivalent time constant, given as $T_0 = t_s\,(2.5 \sim 3) = \mu_1 \mu_0$, furthermore, the recommended standard values of the stability indices are $\gamma_1 = 2.5$, $\gamma_i = 2, i = 2 \sim (n-1), \gamma_0 = \gamma_n = \infty$ and the stability limits are $\gamma_i{}^* = 1\gamma_{i-1} + 1\gamma_{i+1}$ to perform the stability and the shape of the time response, but the robustness is specified by the variation of stability indices due to plant perturbations and parameter variations.
Stability indices are related to the coefficients of characteristic polynomial by $\gamma_i = \mu_i{}^2(\mu_{i-1}\mu_{i+1})$.
The parameters t_s and T_0 can be modified to provide the needed performance, with $\gamma_i > 1.5\gamma_i{}^*$ for all $i = 1 \sim (n-1)$. When the prefilter $F(s) = P(s)|_{s=0}\, N(s)$ is chosen to decrease the steady-state error to zero (Coelho et al. 2016).

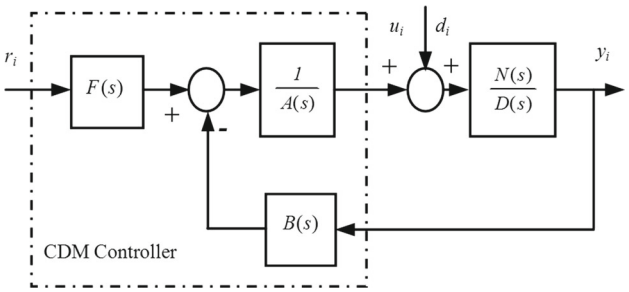

Fig. 1 Block scheme of the CDM control

4 Disturbance Observer-Based CDM-Backstepping

Backstepping technique is a recursive procedure that the Lyapunov function is used with the design of feedback control (Chaoui and Gualous 2017; Chihab et al. 2015; Benslimane et al. 2017; Ting et al. 2016). The n-order system is divided into n subsystems and is taken one of the states of the second subsystem as the control of the first subsystem; this state is replaced by the desired control and a new virtual state (Chen et al. 2016; Nguyen et al. 2019; Pratap and Purwar 2014). Continuing backstepping until the last subsystem, all shifted nonlinearities can be cancelled by the actual control (Ahn et al. 2014).

In this section the robust CDM-backstepping is proposed step by step to control the angular displacement of an EHSS which yields external disturbance and noise rejections. In this work, the use of an observer is necessary to estimate the disturbance d of the friction and load force, where the stability is proven by Lyapunov theorem.
From the dynamics model of EHSS system, it can be formulated d as $d = -m\dot{x}_2 + A_p x_3 - f_1$.
The estimations of the disturbance $\hat{d}$ are defined. The estimation error is specified as $e_d = d - \hat{d}$, and the dynamic of $\hat{d}$ can be obtained as

$\dot{\hat{d}} = -l_o \left(m\dot{x}_2 - A_p x_3 + f_1 + \hat{d} \right)$. where the observer gain is represented by l_o, and the disturbance and its time derivative are bounded, where $|\dot{d}| \le \dot{d}_{max}$.
The auxiliary variable is assumed $\xi = -\hat{d} - l_o m x_2$; then, the time derivative of ξ is taken, $\dot{\xi} = -\dot{\hat{d}} - l_o m \dot{x}_2$. It can be specified as

$$\dot{\xi} = -l_o \left(\xi + l_o m x_2 \right) + l_o \left(-A_p x_3 + f_1 \right) \tag{4}$$

The estimation error can be taken such that $\dot{e}_d = -l_o e_d + \dot{d}$ with $e_d \le \exp(-l_o t).|e_d(0)| + 1 l_o \rho(t)$ and $\rho(t) \ge |\dot{d}|$, $\forall t \ge 0$.

Firstly, the error z_1 is taken $z_1 = x_1 - x_d$, and the first Lyapunov function is defined as $V_1 = 0.5{z_1}^2$, its derivative with respect to time is specified as $\dot{V}_1 = z_1\dot{z}_1$, and this can be written as : $\dot{V}_1 = z_1(x_2 - \dot{x}_d)$, after that the error z_2 is taken : $z_2 = x_2 - \dot{x}_d - \phi_1$, $\dot{V}_1$ is obtained as $\dot{V}_1 = z_1(z_2 + \phi_1) = z_1(z_2 - k_1 z_1) = -k_1{z_1}^2 + z_1 z_2$.
Let the second Lyapunov function V_2 is as follows $V_2 = V_1 + 0.5{z_2}^2 + 0.5{e_d}^2$, and its time derivative can be expressed as $\dot{V}_2 = \dot{V}_1 + z_2\dot{z}_2 + e_d\dot{e}_d$ then, taking $\dot{z}_2 = \dot{x}_2 - \ddot{x}_d - \dot{\phi}_1$, consequently

$$\begin{aligned}\dot{V}_2 &= \dot{V}_1 + z_2(\dot{x}_2 - \ddot{x}_d - \dot{\phi}_1) + e_d\dot{e}_d \\ &= \dot{V}_1 + z_2\left(\tfrac{A_\mathrm{p}}{m}x_3 - \tfrac{f_1}{m} - \tfrac{d}{m} - \ddot{x}_d - \dot{\phi}_1\right) \\ &\quad + e_d\dot{e}_d \\ &= \dot{V}_1 + z_2\left(\tfrac{A_\mathrm{p}}{m}(z_3 + \ddot{x}_d + \phi_2) - \tfrac{f_1}{m} - \tfrac{d}{m} - \ddot{x}_d - \dot{\phi}_1\right) \\ &\quad + e_d(-l_\mathrm{o}e_d + \dot{d}) \\ &= \dot{V}_1 \\ &\quad + z_2\left(\tfrac{A_\mathrm{p}}{m}z_3 + \tfrac{A_\mathrm{p}-m}{m}\ddot{x}_d + \tfrac{A_\mathrm{p}}{m}\phi_2 - \tfrac{f_1}{m} - \tfrac{d}{m} - \ddot{x}_d - \dot{\phi}_1\right) \\ &\quad + e_d(-l_\mathrm{o}e_d + \dot{d})\end{aligned} \tag{5}$$

ϕ_2 is taken as $\phi_2 = (1A_\mathrm{p})(f_1 - (A_\mathrm{p} - m)\ddot{x}_d - k_2 m z_2 - m z_1 + \hat{d})$, and one has

$$\dot{V}_2 = -k_1{z_1}^2 - k_2{z_2}^2 - \frac{1}{m}z_2e_d + \frac{A_\mathrm{p}}{m}z_2z_3 + e_d(-l_\mathrm{o}e_d + \dot{d}) \tag{6}$$

Then

$$\begin{aligned}\dot{V}_2 &\le -k_1{z_1}^2 - k_2\left({z_2}^2 + \tfrac{1}{k_2 m}z_2e_d\right) \\ &\quad + \tfrac{A_\mathrm{p}}{m}z_2z_3 - l_o{e_d}^2 + |e_d|\,|\dot{d}| \\ &= -k_1{z_1}^2 - k_2\left(z_2 + \tfrac{1}{2k_2 m}e_d\right)^2 + \tfrac{A_\mathrm{p}}{m}z_2z_3 \\ &\quad - \eta\left(|e_d| - \tfrac{1}{2\eta}|\dot{d}|\right)^2 + \tfrac{1}{4\eta}|\dot{d}|^2 \\ &\le -k_1{z_1}^2 - k_2\left(z_2 + \tfrac{1}{2k_2 m}e_d\right)^2 + \tfrac{A_\mathrm{p}}{m}z_2z_3 \\ &\quad - \eta\left(|e_d| - \tfrac{1}{2\eta}|\dot{d}_\mathrm{max}|\right)^2 + \tfrac{1}{4\eta}\dot{d}_\mathrm{max}^2\end{aligned} \tag{7}$$

The third Lyapunov function is taken as $V_3 = V_2 + 0.5{z_3}^2$, subsequently $\dot{V}_3 = \dot{V}_2 + z_3\dot{z}_3$, z_3 is selected as $z_3 = x_3 - \ddot{x}_d - \phi_2$, at that time $\dot{z}_3 = \dot{x}_3 - \dddot{x}_d - \dot{\phi}_2$, and consequently :

$$\begin{aligned}\dot{V}_3 &= \dot{V}_2 + z_3(\dot{x}_3 - \dddot{x}_d - \dot{\phi}_2) \\ &= \dot{V}_2 + z_3(a_2x_2 + a_3x_3 + bx_4 - \dddot{x}_d - \dot{\phi}_2)\end{aligned} \tag{8}$$

Then, z_4 is taken as $z_4 = x_4 - \dddot{x}_d - \phi_3$, and as a consequence $\dot{V}_3 = \dot{V}_2 + z_3(a_2x_2 + a_3x_3 + b(z_4 + \ddot{x}_d + \phi_3) - \dddot{x}_d - \dot{\phi}_2)$, as well $\dot{V}_3 = \dot{V}_2 + z_3(a_2x_2 + a_3x_3 + bz_4 + (b-1)\ddot{x}_d + b\phi_3 - \dot{\phi}_2)$.

In that case, ϕ_3 is chosen as $\phi_3 = (1b)(-a_2x_2 - a_3x_3 - (b-1)\dddot{x}_d + \dot{\phi}_2 - k_3z_3 - (A_\mathrm{p}m)z_2)$; then,

$$\begin{aligned}\dot{V}_3 \le{}& -k_1z_1^2 - k_2\left(z_2 + \tfrac{1}{2k_2m}e_d\right)^2 - \eta\left(|e_d| - \tfrac{1}{2\eta}\dot{d}_\mathrm{max}\right)^2 \\ &+ \tfrac{1}{4\eta}\dot{d}_\mathrm{max}^2 - k_3z_3^2 + bz_3z_4\end{aligned} \tag{9}$$

The fourth Lyapunov function is designed as $V_4 = V_3 + 0.5{z_4}^2$, its time derivative is given by $\dot{V}_4 = \dot{V}_3 + z_4\dot{z}_4$, after that z_4 is defined as $z_4 = x_4 - \ddot{x}_4 - \phi_3$, also $\dot{z}_4 = x_5 - \dddot{x}_4 - \dot{\phi}_3$, then

$$\dot{V}_4 = \dot{V}_3 + z_4(\dot{x}_4 - \ddot{x}_4 - \dot{\phi}_3) = \dot{V}_3 + z_4(x_5 - \ddot{x}_4 - \dot{\phi}_3) \tag{10}$$

where

$$z_5 = x_5 - \ddot{x}_4 - \phi_4 \tag{11}$$

The time derivative of V_4 is specified as $\dot{V}_4 = \dot{V}_3 + z_4(z_5 + \phi_4 - \dot{\phi}_3)$, and ϕ_4 is taken $\phi_4 = \dot{\phi}_3 - k_4z_4 - bz_3$, and one has :

$$\begin{aligned}\dot{V}_4 \le{}& -k_1z_1^2 - k_2\left(z_2 + \frac{1}{2k_2m}e_d\right)^2 - \eta\left(|e_d| - \frac{1}{2\eta}\dot{d}_\mathrm{max}\right)^2 \\ &+ \frac{1}{4\eta}\dot{d}_\mathrm{max}^2 - k_3z_3^2 - k_4z_4^2 + z_4z_5\end{aligned}$$

The final Lyapunov function is designed as follows $V_5 = V_4 + 0.5z_5^2$, then $\dot{V}_5 = \dot{V}_4 + z_5\dot{z}_5$, and one has

$$\begin{aligned}\dot{V}_5 \le{}& -k_1z_1^2 - k_2\left(z_2 + \tfrac{1}{2k_2m}e_d\right)^2 - \eta\left(|e_d| - \tfrac{1}{2\eta}\dot{d}_\mathrm{max}\right)^2 \\ &+ \tfrac{1}{4\eta}\dot{d}_\mathrm{max}^2 - k_3z_3^2 - k_4z_4^2 + z_4z_5 + z_5\dot{z}_5\end{aligned} \tag{12}$$

where $\dot{z}_5 = \dot{x}_5 - \dddot{x}_4 - \dot{\phi}_4$.
The virtual control is defined as $\zeta = x_5$; then, the control signal is expressed as follows

$$a_{\mathrm{o}0}(x)u + a_{\mathrm{o}1}(x)\frac{\mathrm{d}u}{\mathrm{d}t} = e_\mathrm{o}(t) \tag{13}$$

where

$$e_\mathrm{o}(t) = c_{\mathrm{o}0}(x)\phi_4 - b_{\mathrm{o}0}(x)\zeta - b_{\mathrm{o}1}(x)\dot{\zeta} \tag{14}$$

$a_{\mathrm{o}0}(x)$, $a_{\mathrm{o}1}(x)$, $c_{\mathrm{o}0}(x)$, $b_{\mathrm{o}0}(x)$ and $b_{\mathrm{o}1}(x)$ are nonlinear gains of nonlinear coefficient diagram method controller presented in (13)–(14).

Consider the electrohydraulic servo system dynamic specified by (1) with coefficient diagram method control (13)–(14), and that the gains δ_o and c_o are assumed such that

$$\left| c_o \delta_o \text{sign}(z_o) \int_0^t z_5(\sigma) d\sigma \right| > \Delta_o \quad \text{with} \quad \Delta_o \geq |z_4| + |h(x)| \tag{15}$$

The errors $z_5(t)$ are obliged by the control signal to converge to zero that will be now defined. Firstly the next nonlinear gains are selected as

$$\begin{cases} a_{o0}(x) = -k_o \, (da_6 dt) = 0 \\ a_{o1}(x) = -k_o a_6. \end{cases} \tag{16}$$

With k_o is any positive constant. Then, Eq. (11) is substituted into (14); it is given $z_5 = \left(b_{0o}^{-1} c_{0o} - 1\right) \phi_4 - b_{0o}^{-1} e_o$ and the next nonlinear gains are taken $c_{o0}(x) = b_{o0}(x) = c_o$ and $b_{o1}(x) = 0$, then

$$e_o = -c_o z_5 \tag{17}$$

Its second derivative with respect to time is expressed as

$$\ddot{e}_o = c_o \ddot{\phi}_4 - c_o \ddot{\xi} + c_o \dddot{x}_4 \tag{18}$$

Equations (13), (14) and (16) are combined and yield

$$\ddot{\xi} = \dot{f}_3 - k_{o1} e_o \tag{19}$$

With $k_{o1} = {k_o}^{-1}$ after that, Eq. (19) is substituted into (18), and it is obtained $\ddot{e}_o = c_o \ddot{\phi}_4 - c_o(\dot{f}_3 - k_{o1} e_o) + c_o \dddot{x}_4$, then

$$\dot{e}_o = c_o \dot{\phi}_4 - c_o \left(f_3 - k_{o1} \int_0^t e_o(\sigma) d\sigma \right) + c_o \ddot{x}_4 \tag{20}$$

And Eq. (17) is used to find

$$\dot{z}_5 = h_o(x) - k_{o1} \int_0^t e_o(\sigma) d\sigma \tag{21}$$

With $h_o(x) = f_3 - \dot{\phi}_4(t) - \ddot{x}_4(t)$, then taking $k_{o1} = \delta_o \text{sign}(z_o)$ and $z_o = z_5 \int_0^t z_5(\sigma) d\sigma$, then replacing the dynamics of z_5 given by (21) and the control signal specified by (13), next one has

$$\begin{aligned} \dot{V}_5 \leq & -k_1 z_1^2 - k_2 \left(z_2 + \tfrac{1}{2k_2 m} e_d \right)^2 - \eta \left(|e_d| - \tfrac{1}{2\eta} \dot{d}_{\max} \right)^2 \\ & + \tfrac{1}{4\eta} \dot{d}_{\max}^2 - k_3 z_3^2 - k_4 z_4^2 + v_o(t) \end{aligned} \tag{22}$$

where $v_o(t) = z_5 \left(z_4 + h_o(x) - k_{o1} \int_0^t z_5(\sigma) d\sigma \right)$, then $\dot{V}_5$ is written as $\dot{V}_5 \leq -(1-\varsigma)\dot{V}_{50} - \varsigma \dot{V}_{50} + \frac{1}{4\eta} \dot{d}_{\max}^2 + v_o(t)$ with : $\dot{V}_{50} = k_1 z_1^2 + k_2 \left(z_2 + \frac{1}{2k_2 m} e_d \right)^2 + \eta \left(|e_d| - \frac{1}{2\eta} \dot{d}_{\max} \right)^2 + k_3 z_3^2 + k_4 z_4^2$

and $0 < \varsigma < 1$, if l_o is chosen such that $\frac{1}{l_o} < 4m^2 k_2$ and $\|z_l\| \geq B_l$, where $z_l = [z_1, z_2, z_3, z_4, z_5, e_d]^T$, $B_l = \left\{ z_l \,|\, \varsigma \dot{V}_5 = \frac{1}{4\eta} \dot{d}_{\max}^2 \right\}$, but :

$v_o(t) = z_5 \left(z_4 + h_o(x) - c_o \delta_o z_o sign(z_o) \right)$ is negative, then it is obtained $\dot{V}_5 \leq -(1-\varsigma)\dot{V}_{50}$, and as a result, the tracking errors z_1, z_2, z_3, z_4, z_5 and the disturbance observer error e_d are asymptotically stable.

5 TLBO Algorithm

The key idea of TLBO is the reproduction of a traditional teaching learning method of a classroom between the teacher and the students to search the optimum solution. The algorithm has two phases, the teacher phase and the learner phase (Chatterjee and Mukherjee 2016). Throughout the first phase, the knowledge is instructed by the teacher among the learners and an effort is made to increase the mean result of the class. The knowledge will be gained by learners depending upon the quality of the learners present in the class and the quality of the teaching.

The second phase is the learner phase in which the learner acts as a teacher for other learners and his knowledge is tried to improve by means of interaction. Therefore, their knowledge has been allowed by the learners to improve by interaction if more knowledge has been acquired than him by the other learner.

The subjects are the parameters of the controller CDM-backstepping with disturbance observer, and the teacher/learner with the best performance index is treated as the near-optimum solution. The overall block diagram of the EHSS with the TLBO algorithm is shown in Fig. 2. The convergence of the TLBO algorithm on the way to global optimum solution is supervised by the performance index of the system. As the iteration increased, the parameters of the controller are adapted in such way to produce a minimum performance index.

The following steps are integrated by the TLBO algorithm:

Step 1: In this step the number of students is initialized, and then the objective function is evaluated for each student.

The initial number of students is chosen on the basis of parameters adjusted employing traditional method.

$$\psi_n = \left[\delta_o \; c_o \; l_o \right]_n \tag{23}$$

where n is the number of student in a class.

Step 2: The mean of each student is computed. Then the mean of performance index ITAE $= \int_0^\infty t \, |e(t)| \, dt$ (Bouchebbat and Gherbi 2016; Bourouba et al. 2017; Razmjooy et al.

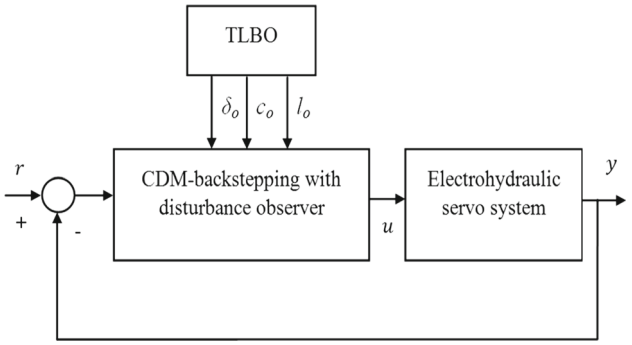

Fig. 2 TLBO tuning approach for CDM-backstepping with disturbance observer

2016) of the generated population is calculated.

$$\Psi_{\text{mean}} = \frac{\sum_{i=1}^{n} \text{ITAE}}{n} \tag{24}$$

Step 3: On the basis of minimum performance index attained, the best student is detected

$$\Psi_{\text{best}} = \left[\delta_{\text{o}}\ c_{\text{o}}\ l_{\text{o}}\right]_{\min \text{ITAE}} \tag{25}$$

In addition, the teaching factor is determinate so that the best student would operate as a teacher for the next iteration.

$$\text{TF} = \frac{\sum_{i=1}^{n} \text{ITAE} - n}{\sum_{i=1}^{n} \text{ITAE} - \min(\text{ITAE})} \tag{26}$$

Step 4: For all students, the learners' knowledge acquired by the acting teacher is updated as follows

$$\Psi_{\text{new}} = \Psi_{\text{old}} + r\,(\Psi_{\text{best}} - TF \times \Psi_{\text{mean}}) \tag{27}$$

where $r \in \left[0\ 1\right]$ is the random variable.
For these updated parameters, the performance index is computed and compared with the ITAE of old students. If new parameters are better than the preceding one, then it is kept for next iteration; otherwise, it is excluded.
Step 5: Any two variables from Ψ_{new} are chosen randomly, and her performance index is compared with the performance index of these of each student. If $\Psi_{\text{new}i}$ is better, then $\Psi_{\text{new}j}$:

$$\left\{\begin{array}{l} \psi_{\text{new}} = \Psi_{\text{old}} + r\,(\Psi_{\text{newi}} - \Psi_{\text{new}}) \\ \text{else} \\ \Psi_{\text{new}} = \Psi_{\text{old}} + r\left(\Psi_{\text{newj}} - \Psi_{\text{newi}}\right) \end{array}\right\} \tag{28}$$

Step 6: The updated learners' knowledge is saved, and their performance index is compared with the current one. The new learners' knowledge is selected if they are better in the sense of ITAE; otherwise, the preceding solution is accomplished for next iteration. The process is ended if the design requirements are satisfied.

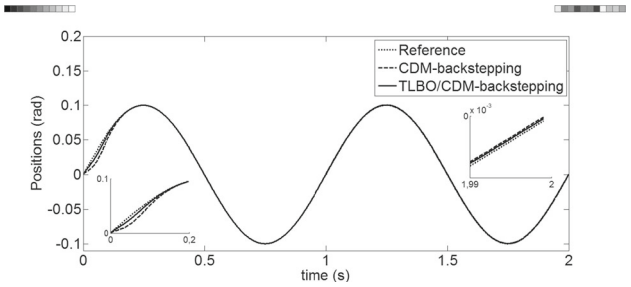

Fig. 3 CDM-backstepping control, position tracking performance

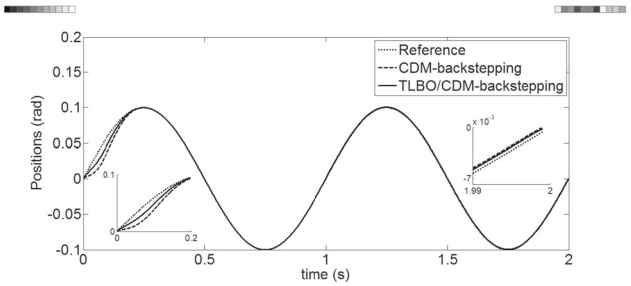

Fig. 4 CDM-backstepping with disturbance observer, position tracking performance

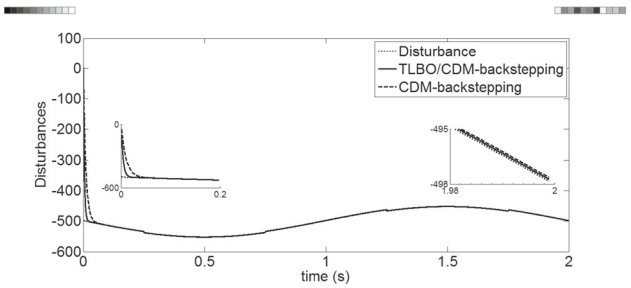

Fig. 5 Estimation performance of disturbance

6 Computer Simulation

In this section, the parameters of the combined CDM-backstepping and disturbance observer are adjusted by using TLBO algorithm. Firstly the parameters are randomly designated using trial and error method. For TLBO algorithm, the number of students is selected twenty. The performance is computed for every parameter of controller. The parameters of the EHSS are set as follows :

$$\begin{aligned} &m = 0.29\ \text{kg},\ A_{\text{p}} = 6.032 \times 10^{-4}\ \text{m}^2,\ \rho = 870\ \text{kg/m}^3, \\ &V_{\text{t}} = 6.6 \times 10^{-6}\ \text{m}^3,\ C_{\text{d}} = 0.62,\ K_{\text{s}} = 5 \times 10^{-5}\ \text{N/m}, \\ &B = 830\ \text{N/(m/s)},\ \beta_{\text{e}} = 7 \times 10^{8}\ \text{N/m}^2,\ \omega = 0.0314\,\text{m}, \\ &\zeta_{\text{sv}} = 0.6,\ C_{\text{tp}} = 8 \times 10^{12}\ \text{m}^5/(\text{N s}),\ K_{\text{sv}} = 0.0075\,\text{m/A}, \\ &K_{\text{a}} = 0.001\text{A/V},\ P_{\text{s}} = 11 \times 10^{6}\ \text{Pa},\ \omega_{\text{sv}} = 282\ \text{rad/s}. \end{aligned}$$

Test one Unknown disturbance

Simulation results are shown in Figs. 3, 4, 5, and the unknown disturbance in friction and load force is taken : $d = -500 - 50\sin(\pi t) + 2\text{sign}(x_2)$, where $d(0) = -500$, $\hat{d}(0) = 0$ and $x(0) = [0\ 0\ 0\ 0]^T$. The corresponding performance index in terms of ITAE value and settling time is shown in Table 1. It is clear that, with the proposed TLBO technique, minimum ITAE value ($= 0.06\times10^{-5}$) is obtained compared to conventional approach ($= 3.1 \times 10^{-5}$), Also a satisfactory transient behavior is produced by the optimized controller, without overshoot and shorten settling time about 0.09 s, and it can be noticed that the maximum value of the position error is approximately zero at steady state. Consequently, better system performance is achieved with proposed optimized controller. From the above analysis it is shown that the system performance is improved by applying the proposed approach. Also it is shown in Figs. 3 and 4 that better performance than conventional CDM-backstepping is exhibited by the optimized controller. It is indicated in Fig. 5 that the unknown disturbance was well estimated using the optimized controller.

Test two Measurement noise

To evaluate the performance of the optimized disturbance observer based on CDM-backstepping in the presence of a measurement noise, the disturbance estimation performance was compared with the conventional controller; from Fig. 6, it can be seen that the estimated disturbances of the conventional approach had large ripples; however, the optimized approach had small ripples in the estimated disturbances. So we can conclude that the measurement noises produced in the sensors can be reduced; then, better dynamic performance of the disturbance estimation is obtained with proposed TLBO optimized controller. So, it can be concluded that the performance of proposed control with TLBO algorithm is superior than conventional controller algorithms.

Test three Uncertainties

In order to evaluate the performance of the proposed control algorithms against uncertainties; parameter uncertainties are added to the system. Figures 7 and 8 show the position tracking of the two methods and the estimation performances of the disturbance. Due to the parameter uncertainties, the position tracking performance of the conventional control was the worst and did not satisfy the position tracking with shorten settling time and converge with large steady-state error in comparing with the result obtained from the optimized controller, also the disturbances were well estimated

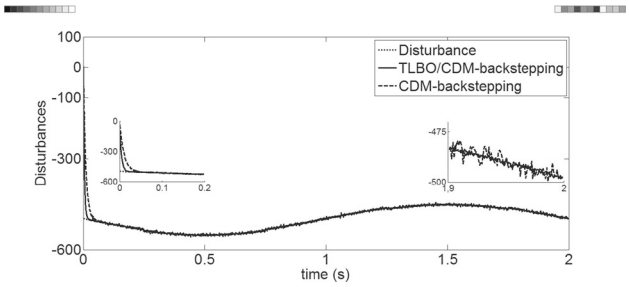

Fig. 6 Disturbance estimation performance with measurement noises

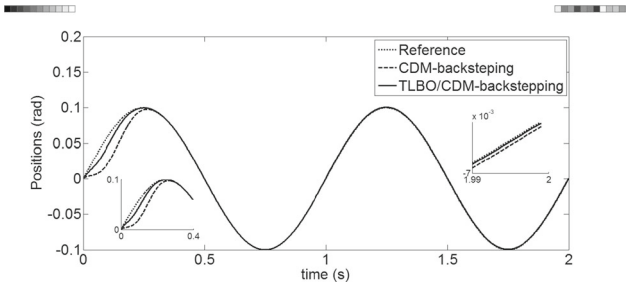

Fig. 7 CDM-backstepping with disturbance observer, position tracking performance

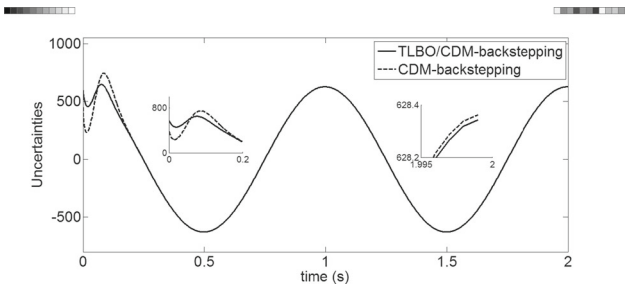

Fig. 8 Disturbance estimation performance with uncertainties

with the optimized method, so that the proposed method has the best position tracking performance among the conventional method.

We can conclude that the proposed controller is highly improved by TLBO and can show its proficient against unknown disturbance, measurement noise and uncertainties.

7 Conclusion

The TLBO method is used to tune the parameters of the integrated disturbance observer and CDM-backstepping con-

Table 1 The comparison of each algorithm performance

Algorithms	Ψ	$t_s(s)$	ITAE
Conventional CDM-backstepping	[32 0.29 2.1]	0.12	3.1×10^{-5}
TLBO/CDM-backstepping	[22 0.26 1.54]	0.09	0.06×10^{-5}

troller for guarantying high performance in position tracking of the EHSS. The optimal parameters are tuned by the presented TLBO technique where the objective function of the desired performance is minimized. The effectiveness of the suggested optimization technique under noise, external disturbance and parameters uncertainties was proven by making comparison between conventional CDM-backstepping and TLBO/CDM-backstepping, Furthermore, it can be decided that the offered controller has more robustness and performance characteristics than the traditional controller.

References

Abtahi, S. F., & Yazdi, E. A. (2019). Robust control synthesis using coefficient diagram method and μ-analysis: An aerospace example. *International Journal of Dynamics and Control*,. https://doi.org/10.1007/s40435-018-0462-7.

Ahn, K. K., Nam, D. N. C., & Jin, M. (2014). Adaptive backstepping control of an electrohydraulic actuator. *IEEE/ASME Transactions on Mechatronics*,. https://doi.org/10.1109/TMECH.2013.2265312.

Ali, H., Magdy, G., Li, B., Shabib, G., Elbaset, A. A., Xu, D., et al. (2019). A new frequency control strategy in an islanded microgrid using virtual inertia control-based coefficient diagram method. *IEEE Access*,. https://doi.org/10.1109/ACCESS.2019.2894840.

Arsalan, M., Iftikhar, R., Ahmad, I., Hasan, A., Sabahat, K., & Javeria, A. (2018). MPPT for photovoltaic system using nonlinear backstepping controller with integral action. *Solar Energy*,. https://doi.org/10.1016/j.solener.2018.04.061.

Ba, D. X., Ahn, K. K., Truong, D. Q., & Park, H. G. (2016). Integrated model-based backstepping control for an electro-hydraulic system international. *Journal of Precision Engineering and Manufacturing*,. https://doi.org/10.1007/s12541-016-0069-x.

Baek, S. G., Ji, S., & Koo, J. C. (2018). Experimental study of electro-hydraulic actuator with payload for precision motion control. *Microsystem Technologies*,. https://doi.org/10.1007/s00542-016-3050-9.

Benslimane, H., Boulkroune, A., & Chekireb, H. (2017). Adaptive iterative learning control of nonlinearly parameterized pure feedback nonlinear systems. *Journal of Control, Automation and Electrical Systems*,. https://doi.org/10.1007/s40313-017-0316-0.

Bouchebbat, R., & Gherbi, S. (2016). A novel optimal control and management strategy of stand-alone hybrid PV/wind/diesel power system. *Journal of Control, Automation and Electrical Systems*,. https://doi.org/10.1007/s40313-016-0290-y.

Bourouba, B., Ladaci, S., & Chaabi, A. (2017). Reduced-order model approximation of fractional-order systems using differential evolution algorithm. *Journal of Control, Automation and Electrical Systems*,. https://doi.org/10.1007/s40313-017-0356-5.

Chaoui, H., & Gualous, H. (2017). Adaptive fuzzy logic control for a class of unknown nonlinear dynamic systems with guaranteed stability. *Journal of Control, Automation and Electrical Systems*,. https://doi.org/10.1007/s40313-017-0342-y.

Chatterjee, S., & Mukherjee, V. (2016). PID controller for automatic voltage regulator using teaching-learning based optimization technique. *Electrical Power and Energy Systems*,. https://doi.org/10.1016/j.ijepes.2015.11.010.

Chen, F., Lei, W., Zhang, K., Tao, G., & Jiang, B. (2016). A novel nonlinear resilient control for a quadrotor UAV via backstepping control and nonlinear disturbance observer. *Nonlinear Dynamic*,. https://doi.org/10.1007/s11071-016-2760-y.

Chihab, A. A., Ouadi, H., Giri, F., & Majdoub, K. E. (2015). Adaptive backstepping control of three-phase four-wire shunt active power filters for energy quality improvement. *Journal of Control, Automation and Electrical Systems*,. https://doi.org/10.1007/s40313-015-0221-3.

Coelho, J. P., Pinho, T. M., & Boaventura, C. J. (2016). Controller system design using the coefficient diagram method. *Arabian Journal for Science and Engineering*,. https://doi.org/10.1007/s13369-016-2235-y.

Dashkovskiy, S. N., & Pavlichkov, S. S. (2017). Integrator backstepping for uncertain nonlinear systems with non-smooth dynamics. *European Journal of Control*,. https://doi.org/10.1016/j.ejcon.2017.12.002.

Detiček, E., & Kastrevc, M. (2016). Design of Lyapunov based nonlinear position control of electrohydraulic servo systems. *Strojniški Vestnik-Journal of Mechanical Engineering*,. https://doi.org/10.5545/sv-jme.2015.2921.

Erkan, K., Yalçin, B. C., & Garip, M. (2017). Three-axis gap clearance I-PD controller design based on coefficient diagram method for 4-pole hybrid electromagnet. *Automatika*,. https://doi.org/10.1080/00051144.2017.1382649.

Has, Z., Rahmat, M. F., Husain, A. R., & Ahmad, M. N. (2015). Robust precision control for a class of electrohydraulic actuator system based on disturbance observer. *International Journal of Precision Engineering and Manufacturing*,. https://doi.org/10.1007/s12541-015-0230-y.

Mohamed, T. H., Shabib, G., & Ali, H. (2016). Distributed load frequency control in an interconnected power system using ecological technique and coefficient diagram method. *Electrical Power and Energy Systems*,. https://doi.org/10.1016/j.ijepes.2016.04.023.

Nguyen, T. V., Thai, N. H., Pham, H. T., Phan, T. A., Nguyen, L., Le, H. X., et al. (2019). Adaptive neural network-based backstepping sliding mode control approach for dual-arm robots. *Journal of Control, Automation and Electrical Systems*,. https://doi.org/10.1007/s40313-019-00472-z.

Pratap, B., & Purwar, S. (2014). Real-time implementation of neuro adaptive observer-based robust backstepping controller for twin rotor control system. *Journal of Control, Automation and Electrical Systems*,. https://doi.org/10.1007/s40313-013-0098-y.

Razmjooy, N., Khalilpour, M., & Ramezani, M. (2016). A new meta-heuristic optimization algorithm inspired by FIFA world cup competitions: Theory and its application in PID designing for AVR system. *Journal of Control, Automation and Electrical Systems*,. https://doi.org/10.1007/s40313-016-0242-6.

Sahu, R. K., Panda, S., Rout, U. K., & Sahoo, D. K. (2016). Teaching learning based optimization algorithm for automatic generation control of power system using 2-DOF PID controller. *Electrical Power and Energy Systems*,. https://doi.org/10.1016/j.ijepes.2015.11.082.

Sheng, Z., & Li, Y. (2016). Hybrid robust control law with disturbance observer for high-frequency response electro-hydraulic servo loading system. *Applied Sciences*,. https://doi.org/10.3390/app6040098.

Shoja-Majidabad, S. (2016). Robust rejection of matched/unmatched perturbations from fractional-order nonlinear systems. *Journal of Control, Automation and Electrical Systems*,. https://doi.org/10.1007/s40313-016-0260-4.

Ting, C. S., Lieu, J. F., Liu, C. S., & Hsu, R. W. (2016). An adaptive FNN control design of PMLSM in stationary reference frame. *Journal of Control, Automation and Electrical Systems*,. https://doi.org/10.1007/s40313-016-0243-5.

Vieira, R. P., Gabbi, T. S., & Gründling, H. A. (2017). Combined discrete-time sliding mode and disturbance observer for current control of induction motors. *Journal of Control, Automation and Electrical Systems*,. https://doi.org/10.1007/s40313-017-0307-1.

Wang, W., & Wang, B. (2017). Disturbance observer-based nonlinear energy-saving control strategy for electro-hydraulic servo systems. *Advances in Mechanical Engineering*,. https://doi.org/10.1177/1687814017705842.

Yuan, H.-B., Na, H.-C., & Kim, Y.-B. (2018). Robust MPC–PIC force control for an electro-hydraulic servo system with pure compressive elastic load. *Control Engineering Practice*,. https://doi.org/10.1016/j.conengprac.2018.07.009.